Letter | Editors' Suggestion

Engineering topology in graphene with chiral cavities

Ceren B. Dag [1,2,*] and Vasil Rokaj [1,2,†]

[1]*ITAMP, Harvard-Smithsonian Center for Astrophysics, Cambridge, Massachusetts 02138, USA*

[2]*Department of Physics, Harvard University, Cambridge, Massachusetts 02138, USA*

(Received 26 November 2023; revised 12 March 2024; accepted 16 August 2024; published 3 September 2024)

Strongly coupling materials to cavity fields can affect their electronic properties altering the phases of matter. We study monolayer graphene whose electrons are coupled to both left and right circularly polarized vacuum fluctuations, and time-reversal symmetry is broken due to a phase shift between the two polarizations. We develop a many-body perturbative theory, and derive cavity-mediated electronic interactions. This theory leads to a gap equation which predicts a topological band gap at Dirac nodes in vacuum and when the cavity is prepared in an excited Fock state. Remarkably, topological band gaps also open in light-matter hybridization points away from the Dirac nodes giving rise to photoelectron bands with high Chern numbers. We reveal that the physical mechanism behind this phenomenon is generic and due to the exchange of photons with electronic matter at the hybridization points. Specifically, the number and polarization of exchanged photons directly determine the band topology of graphene subject to enhanced chiral vacuum fluctuations. Hence, our theory shows that graphene-based materials could host Chern insulator phases in engineered electromagnetic environments, bridging cavity quantum electrodynamics to Floquet engineering of materials while protected from the ensuing heating effects.

DOI: 10.1103/PhysRevB.110.L121101

Driving quantum materials by classical light is a mature field of physics [1,2] where one can engineer the band topology of materials [3–11]. Meanwhile, great progress has been achieved in the manipulation of quantum materials with cavity vacuum fields [12–30]. Notably, modifications in the magnetotransport properties [31] and the Hall conductivity [32] due to cavity vacuum fluctuations were reported in experiments, as well as a shift in the critical temperature for the metal-to-insulator transition in $1T$-TaS_2 [33]. Recently, Ref. [16] discussed an experimentally realizable path to chiral cavities through the Faraday effect [34,35]. Specifically, a magneto-optical material coated mirror would induce a phase shift between the two polarizations of the electromagnetic cavity field [36,37] where the phase shift is proportional to the external magnetic field, coating thickness, and the Verdet constant [38]. Such Faraday rotators [36] and metamaterial coated mirrors [39] were also experimentally demonstrated to selectively absorb one polarization or the other, potentially leading to single-polarization chiral cavities. Alternative to an external magnetic field, spontaneous material magnetism can be utilized for Faraday effect [40,41].

Here, we theoretically study a model where a graphene monolayer is coupled to a chiral cavity field with single or two circular polarizations. For the latter, the time-reversal symmetry (TRS) can be broken as a result of an imperfect phase shift with a Faraday mirror, so that one of the polarizations is not eliminated, but only suppressed. In such a setup, what breaks the TRS is the unequal light-matter couplings induced by the two polarizations of the same cavity mode. Hence this Letter generalizes the model previously studied by Refs. [20–22] which omits one polarization to simplify the theoretical treatment.

We formulate a many-body perturbative theory for the continuum Dirac Hamiltonian coupled to light, based on the Schrieffer-Wolff (SW) transformation [42,43], and obtain the cavity-mediated electronic interactions. Then, we apply Hartree-Fock mean-field theory (MFT) and show that the cavity-mediated interactions break TRS, and hence open a topological gap. Further, we derive the gap equations at finite temperature for a cavity either in vacuum or in a Fock state with low photon number. The perturbative treatment captures the numerically predicted enhancement of the gap with the number of chiral photons when the cavity is prepared in a Fock state [44]. By also deriving a minimally coupled tight-binding (TB) Hamiltonian for this setup and examining the band structure, we show that our results remain valid within the microscopic theory. We find that the single-polarization model [20–22] overestimates the Dirac gap in vacuum when Faraday rotation cannot eliminate one of the polarizations.

A central finding of our work is that the light-matter avoided crossings emerging away from the Dirac nodes also acquire a topological character by contributing a nonzero Berry phase to the band wave functions and giving rise to higher Chern bands. We unveil the mechanism behind this phenomenon based on the chiral photon exchange processes with matter, and find that the number and polarization of the exchanged photons determine the topology of the photoelectron bands. Although graphene coupled to a chiral cavity has been recently studied in multiple works [19–22], the focus was entirely on the Dirac nodes in vacuum missing how the quantum nature of the photons affects the Berry phase of the strongly correlated photoelectron wave function away from the Dirac nodes. This fundamental relation also

*Contact author: ceren.dag@cfa.harvard.edu

†Contact author: vasil.rokaj@cfa.harvard.edu

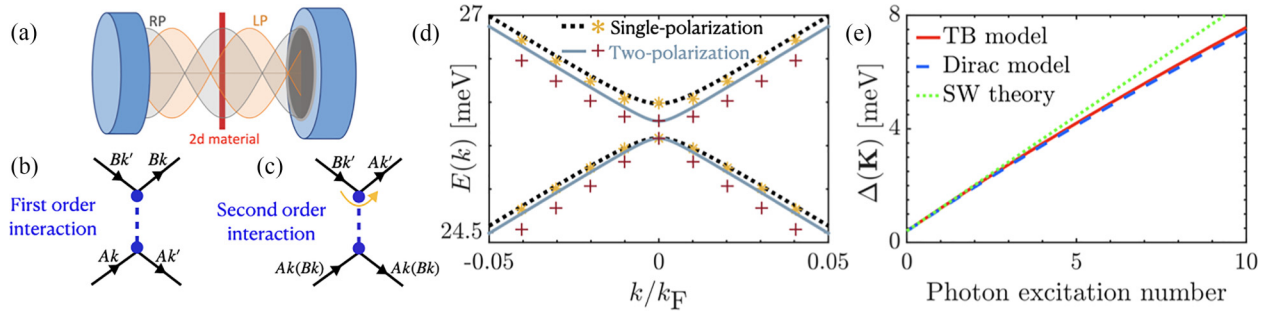

FIG. 1. (a) Chiral cavity setup with right and left polarizations are shifted with respect to each other. (b), (c) The cavity-mediated electronic interactions in graphene with strengths proportional to (b) $1/\omega_\lambda$ and (c) $1/\omega_\lambda^2$. (d) The focus on the lowest two bands of two- and single-polarization Dirac models showing the match between analytical SW theory and exact diagonalization (ED) with a truncated photonic Hilbert space of maximum photon number $\langle a_j^\dagger a_j\rangle_{\max} = 4$. Single-polarization bands (dotted black) are shifted upwards for comparison by $\omega_L/2$. The x axis is defined in terms of radial distance to the Dirac nodes $k = \sqrt{k_x^2 + k_y^2}$ normalized by Fermi momentum $k_F = m v_F$. The parameters are $\omega_c = 6.28$ THz, $\chi = 5 \times 10^{-4}$ [31], and $m = 0.02 m_e$. The Fermi velocity is found to be $v_F = 0.21$ a.u. (atomic units) by fitting the band structure of the Dirac model to the TB model. The red pluses and yellow stars are the prediction of the analytical SW theory in vacuum. (e) The gap at the **K** point when the cavity is prepared in a Fock state, increases with the photon number populated in the cavity. SW theory can predict the gap until $\langle a_R^\dagger a_R\rangle \sim 5$. The ED results with $\langle a_j^\dagger a_j\rangle_{\max} = 4$ on Dirac and TB models match.

provides a physically intuitive and generic framework to engineer photoelectron bands with arbitrary Chern numbers, as well as a possible microscopic origin of Floquet topological insulators [3] with high Chern numbers [45–47]. Let us note in passing that cavity-QED and Floquet engineering of two-dimensional (2D) materials are separate fields where both aim to use light to control the electronic properties of condensed matter, however, in and out of equilibrium, respectively [16,48].

Cavity-mediated interactions. We consider a graphene monolayer described by the continuum Dirac model [49] placed in a single-mode cavity with frequency ω_c whose polarizations are in plane such that they couple to electrons. The effective Hamiltonian around the **K** valley reads ($\hbar = 1$) [21]

$$\mathcal{H}_{\mathbf{K}} = v_F \sum_{\mathbf{k}} (k_x - A_x + i[k_y - A_y]) c_{A\mathbf{k}}^\dagger c_{B\mathbf{k}} + \text{H.c.} + \sum_{\lambda=R,L} \omega_\lambda \left(a_\lambda^\dagger a_\lambda + \frac{1}{2} \right), \tag{1}$$

where the Fermi velocity $v_F = 0.21$ a.u. is found by comparing the band structure of $\mathcal{H}_{\mathbf{K}}$ to that of the TB model around the Dirac nodes [50]. The operators $c_{r\mathbf{k}}$ are fermionic annihilation operators at $r = A, B$ sublattices with momentum $\mathbf{k}$ obeying $\{c_{r\mathbf{k}}^\dagger, c_{s\mathbf{k}'}\} = \delta_{\mathbf{k}\mathbf{k}'}\delta_{rs}$. The frequencies of the right and left circular polarizations are $\omega_\lambda = \sqrt{\omega_c^2 + \omega_D^2}$ where $\lambda = R, L$ and the diamagnetic frequency ω_D stemming from the $\mathbf{A}^2$ term shifts the cavity frequency ω_c [50]. The quantized vector potential written in terms of the circular polarizations $\mathbf{e}_{R,L} = (1, \pm i)/\sqrt{2}$ is

$$\mathbf{A} = \sqrt{\frac{1}{\epsilon_0 \mathcal{V}_\lambda 2\omega_\lambda}} [\mathbf{e}_R a_L + \mathbf{e}_R a_R^\dagger + \mathbf{e}_L a_R + \mathbf{e}_L a_L^\dagger].$$

$\mathcal{V}_\lambda = \chi_\lambda (2\pi c/\omega_c)^3$ [31] is the effective cavity volume with light concentration parameter χ_λ. Here, the operators $[a_\lambda, a_{\lambda'}^\dagger] = \delta_{\lambda\lambda'}$ are the circularly polarized photon operators renormalized by the diamagnetic $\mathbf{A}^2$ term originating from the minimally coupled TB Hamiltonian [50]. Thus the light-matter interaction Hamiltonian follows as $\mathcal{H}_{\text{int}} = -v_F \sum_{\mathbf{k}} (g_R a_R^\dagger + g_L a_L) c_{A\mathbf{k}}^\dagger c_{B\mathbf{k}} + \text{H.c.}$ The light-matter coupling amplitudes in terms of the microscopic parameters are obtained to be $g_\lambda = \frac{\alpha}{m}\sqrt{2\pi/(\mathcal{V}_\lambda \omega_\lambda)}$ in the TB model derivation [50], where $\alpha = 2.68$ a.u. is the lattice distance and m is the effective mass of the electrons subject to the crystal potential which should be fixed by the experiment [51]. Faraday rotation shifts the circular polarizations with respect to each other [36] giving rise to an out-of-phase spatial profile in the cavity field, as shown in Fig. 1(a). This leads to an asymmetry in the light-matter coupling constants g_λ depending on where the 2D material is placed. We assume $2\chi_R = \chi_L$, and hence $g_R = \sqrt{2} g_L$ for the numerical demonstration, although the physics does not qualitatively change as long as $g_R \neq g_L$ [50].

To derive the cavity-mediated interactions we perform the SW transformation $H_{\mathbf{K}} = e^S \mathcal{H}_{\mathbf{K}} e^{-S}$ [42,43]. The light-matter Hamiltonian $\mathcal{H}_{\mathbf{K}}$ is split into the noninteracting $\mathcal{H}_0$ and interaction part $\mathcal{H}_{\text{int}}$, $\mathcal{H}_{\mathbf{K}} = \mathcal{H}_0 + \mathcal{H}_{\text{int}}$. Then, the operator $S = S_1 + S_2 + \cdots$ is constructed perturbatively as an expansion in orders of $1/\omega_\lambda$, such that the light-matter interaction is eliminated, $[S, \mathcal{H}_0] = -\mathcal{H}_{\text{int}}$ [43]. To first order in this expansion we find [50]

$$S_1 = v_F \sum_{\mathbf{k}} \left(\frac{g_L}{\omega_L} a_L - \frac{g_R}{\omega_R} a_R^\dagger \right) c_{A\mathbf{k}}^\dagger c_{B\mathbf{k}} - \text{H.c.} \tag{2}$$

Given the operator S, we derive the effective SW Hamiltonian $H_{\mathbf{K}} = \mathcal{H}_0 + \frac{1}{2}[S, \mathcal{H}_{\text{int}}]$. For a cavity in vacuum this takes the form of

$$H_{\mathbf{K}} = \frac{\omega_R + \omega_L}{2} + v_F \sum_{\mathbf{k}} \Bigg[(k_x + i k_y) c_{A\mathbf{k}}^\dagger c_{B\mathbf{k}} - \sum_{\mathbf{k}'} \left(\frac{g_R^2}{2\omega_R} c_{B\mathbf{k}}^\dagger c_{A\mathbf{k}} c_{A\mathbf{k}'}^\dagger c_{B\mathbf{k}'} + \frac{g_L^2}{2\omega_L} c_{A\mathbf{k}}^\dagger c_{B\mathbf{k}} c_{B\mathbf{k}'}^\dagger c_{A\mathbf{k}'} \right) + \text{H.c.} \Bigg]. \tag{3}$$

The diagrammatic representation of the interactions is given in Fig. 1(b). One can obtain the effective Hamiltonian at $\mathbf{K}'$ valley $H_{\mathbf{K}'}$ by exchanging the sublattice indices $A \leftrightarrow B$ and momentum $\mathbf{k} \to -\mathbf{k}$ in $H_{\mathbf{K}}$. The cavity-mediated interactions break TRS for $g_R \neq g_L$ which we prove below, and estimate the induced gap by MFT whose details are in the Supplemental Material (SM) [50]. The MFT Hamiltonians read $H^{\text{mft}}_{\mathbf{K}} = \sum_{\mathbf{k}}[v'_F(k_x\sigma_1 + k_y\sigma_2) - d_3(\mathbf{k})\sigma_3] + E_0$ and $H^{\text{mft}}_{\mathbf{K}'} = \sum_{\mathbf{k}}[v'_F(-k_x\sigma_1 + k_y\sigma_2) + d_3(\mathbf{k})\sigma_3] + E_0$ at $\mathbf{K}$ and $\mathbf{K}'$ points, respectively, where $\sigma_{1,2,3}$ are the Pauli matrices. Here, v'_F is the renormalized Fermi velocity, and E_0 is the many-body ground-state energy predicted by the MFT, which matches with the band-structure results [50]. The presence of a nonzero $d_3(\mathbf{k})$ in these MFT equations with a different sign means that the TRS is broken. This cavity-induced gap shows that both Dirac nodes contribute a π Berry phase to the wave function, and hence the band gap is topological. We obtain the gap equations for both polarizations to be

$$\Delta_\lambda(\mathbf{k}) = \frac{g_\lambda^2 v_F^2}{2\omega_\lambda}\left(1 + \Delta_\lambda(\mathbf{k})\frac{\tanh\left(\beta E^\lambda_{\mathbf{k}}/2\right)}{2E^\lambda_{\mathbf{k}}}\right), \tag{4}$$

where $\beta = 1/k_BT$ is the inverse temperature, $E^\lambda_{\mathbf{k}} = \sqrt{v_F'^2(k_x^2 + k_y^2) + [\Delta_\lambda(\mathbf{k})]^2/4}$, and the total band-gap opening due to interactions is $\Delta(\mathbf{k}) \equiv \Delta_R(\mathbf{k}) - \Delta_L(\mathbf{k}) = 2d_3(\mathbf{k})$. Right at the $\mathbf{K}$, $\mathbf{K}'$ points and zero temperature, the gap reads $\Delta(\mathbf{0}) = g_R^2 v_F^2/\omega_R - g_L^2 v_F^2/\omega_L$. Hence, in fact, the condition $g_R \neq g_L$ opens a gap. In the limit $T \to \infty$, the gap reduces to $\Delta(\mathbf{0}) = g_R^2 v_F^2/2\omega_R - g_L^2 v_F^2/2\omega_L$. The general solution at $T = 0$ that is plotted in Fig. 1(d) with red pluses, matches with the band structure of the Dirac model in vacuum. The finite-temperature gap is numerically solved in the SM [50].

The single-polarization limit can be obtained by taking $g_L = 0$ in Eqs. (2) and (3). Due to the relative simplicity of this limit, we derive the SW Hamiltonian up to the second order in the perturbation theory with the additional transformation term $S_2 = g_R v_F^2/\omega_R^2 \sum_{\mathbf{k}}[a_R(k_x + ik_y) - \text{H.c.}](n_{A\mathbf{k}} - n_{B\mathbf{k}})$, and we include higher photon excitations with a cavity prepared in a Fock state, such that $\langle a_R^\dagger a_R\rangle \in \mathbb{N}$, and we find

$$\begin{aligned} H^{\text{sp}}_{\mathbf{K}} = {} & v_F \sum_{\mathbf{k}}\left(1 - \frac{v_F^2 g_R^2}{\omega_R^2}\langle a_R^\dagger a_R\rangle\right)(k_x + ik_y)c^\dagger_{A\mathbf{k}}c_{B\mathbf{k}} + \text{H.c.} \\ & + \omega_R\left(\langle a_R^\dagger a_R\rangle + \frac{1}{2}\right) - \frac{g_R^2 v_F}{\omega_R}\langle a_R^\dagger a_R\rangle\sum_{\mathbf{k}}(n_{B\mathbf{k}} - n_{A\mathbf{k}}) \\ & - \frac{g_R^2 v_F}{2\omega_R}\sum_{\mathbf{k}\mathbf{k}'}\Big(c^\dagger_{B\mathbf{k}}c_{A\mathbf{k}}c^\dagger_{A\mathbf{k}'}c_{B\mathbf{k}'} \\ & + v_F\frac{k_x + ik_y}{\omega_R}(n_{A\mathbf{k}} - n_{B\mathbf{k}})c^\dagger_{A\mathbf{k}'}c_{B\mathbf{k}'} + \text{H.c.}\Big). \end{aligned} \tag{5}$$

The interaction induced in the second order with $\propto 1/\omega_R^2$ in Eq. (5) has a complex amplitude and does not preserve sublattice flavor, as depicted in Fig. 1(c). The gap opening introduced in the first order with Eq. (4) is modified by the photon number

$$\Delta_R(\mathbf{k}) = \frac{g_R^2 v_F^2}{2\omega_R}\left(1 + \Delta_R(\mathbf{k})\frac{\tanh\left(\beta E^R_{\mathbf{k}}/2\right)}{2E^R_{\mathbf{k}}}\right) + 2\frac{g_R^2 v_F}{\omega_R}\langle a_R^\dagger a_R\rangle,$$

and accompanied with the renormalization of the Fermi velocity in the second order,

$$v'_F = v_F\left(1 - \frac{v_F^2 g_R^2}{\omega_R^2}\langle a_R^\dagger a_R\rangle\right). \tag{6}$$

In the single-polarization model, $\Delta(\mathbf{k}) = \Delta_R(\mathbf{k})$ by definition. At zero temperature, the gap at $\mathbf{K}, \mathbf{K}'$ points scales as $\Delta(\mathbf{0}) = (2\langle a_R^\dagger a_R\rangle + 1)g_R^2 v_F^2/\omega_R$ which is compatible with Refs. [21,22] in vacuum. Therefore, populating the cavity does not only increase the topological band gap [Fig. 1(e)], it also flattens the bands around $\mathbf{K}, \mathbf{K}'$ points as is visible in Fig. 2(a). The SW theory predicts the gap until the photon excitation number is $\langle a_R^\dagger a_R\rangle \sim 5$ [Fig. 1(e)]. Let us note that applying MFT to the second-order interaction gives rise to coupled gap equations for v'_F and $\Delta(\mathbf{k})$ whose numerical solutions in generic conditions can be found in the SM [50]. We plot these solutions in Fig. 1(d) in vacuum with yellow stars on the single-polarization Dirac model bands, and see a perfect match. Overall, for a split-ring resonator [52] with $\omega_c = 6.28$ THz cavity frequency—corresponding to a Hartree energy of $\sim 9.5 \times 10^{-4}$ a.u.—, $\chi \sim 10^{-4}$ [31], and $m = 0.007m_e$ [51] where m_e is the bare electron mass, the two-polarization model leads to a 4.3 meV gap in vacuum, which is overestimated by the single-polarization model, 11.5 meV [50]. This overestimation is visualized in Fig. 1(c) for a set of different parameter values, and what the vacuum gap depends on is given in the SM [50]. These gaps may be measured via transport [53], or angle-resolved photoemission spectroscopy [54].

Topological photoelectron bands in graphene. For the following discussion, we numerically calculate the Berry curvature $F_{l,xy}(k_x, k_y)$ over the full Brillouin zone (BZ) of the TB models and the Chern number of a band l [55],

$$C_l = \frac{1}{2\pi}\int_{\text{BZ}} F_{l,xy}(k_x, k_y)dk_xdk_y. \tag{7}$$

The Berry phases at a Dirac node and light-matter avoided crossing are denoted by $\phi_{\text{m},l}$ and $\phi_{\text{p},l}$, respectively for band l. Let us note that all photoelectron Dirac bands plotted in Fig. 2 are cross sections cutting through a Dirac node. Hence, the avoided crossings seen symmetrically placed around the $\mathbf{K}$ point are two points residing on a continuous loop of hybridizations around the $\mathbf{K}$ point [50]. Therefore, $\phi_{\text{p},l}$ counts the Berry phase contribution of all avoided crossings at the same radial distance k/k_{F} to the $\mathbf{K}$ point. The Chern number of the band l is $C_l = \Phi_l/\pi$ where Φ_l is the total Berry phase around one valley.

The lowest band, $l = 1$, has two Dirac nodes each contributing to the winding phase of the wave function $\phi_{\text{m},1} = \Phi_1 = \pi$ leading to a Chern band of $C_1 = 1$ as numerically confirmed. However, a more significant characteristic of graphene coupled to a chiral cavity is the emergence of the topological light-matter hybridizations reminiscent of topological polaritons [56]. All higher-energy bands enjoy additional Berry phases proportional to the exchanged photon number: The gaps closest to the valleys, dotted black lines

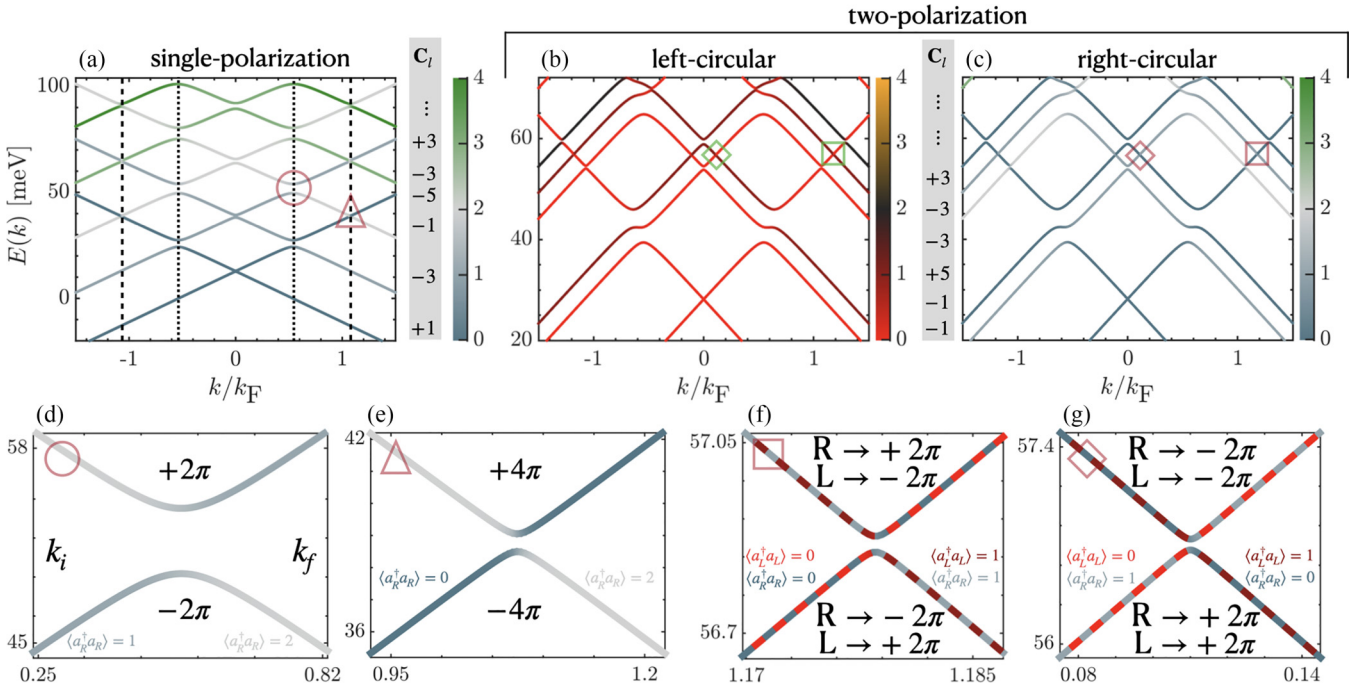

FIG. 2. The exact diagonalization Dirac bands of graphene around the **K** point coupled to a cavity with (a) single polarization and (b), (c) two polarizations of cavity frequency $\omega_c = 6.28$ THz with color coding denoting the photon populations and $\langle a_j^\dagger a_j\rangle_{\max} = 4$. We use $m = 0.02m_e$, $\chi = 5\times10^{-4}$ [31], and $\gamma = 1.2$ as the free parameters of the theory that have to be fixed by the experiment. The light-red shapes highlight the light-matter avoided crossings with chiral photon exchanges. The Chern numbers for both models are given in boxes under $\mathbf{C}_l$ for band l and calculated in the full BZ with the TB model. (d)–(g) Focus on chiral photon exchange processes with Berry phases for each band denoted. The photon numbers are written only for the lower bands. (d) and (e) show the role of photon number, whereas (f) and (g) show also the role of polarization in determining the Berry phase of the photoelectron wave function at a light-matter avoided crossing.

in Fig. 2(a), are one-photon avoided crossings with one chiral photon exchange. This exchange process is enlarged in Fig. 2(d). As a result, the second band gains $\phi_{\mathrm{p},2} = -2\pi$ phase at these one-photon avoided crossings, leading to $\Phi_2 = -3\pi$ total phase together with the $\phi_{\mathrm{m},2} = -\pi$ at the **K** valley giving rise to $C_2 = -3$ as numerically confirmed. The two-photon avoided crossings depicted with dashed black lines in Figs. 2(a) and 2(e), carry the -4π phase for $l = 3$. Therefore, each higher-energy band has an additional loop of light-matter avoided crossings with a phase proportional to $\phi_{\mathrm{p},l} = -2\pi(\langle a_R^\dagger a_R\rangle_l^{k_f} - \langle a_R^\dagger a_R\rangle_l^{k_i})$ contributing to Φ_l, and hence to the Chern number of the band l, where $|k_f| > |k_i|$ is set as the convention. Berry curvature supports this mechanism (see SM [50]).

Polarization of the exchanged photons also affects the Berry curvature and the Chern number of the photoelectron band. Here, we consider a two-polarization model and adopt an alternative mechanism to break TRS through a frequency splitting between two polarizations $\omega_R \neq \omega_L$. This model might be realized either via Zeeman splitting [20,57] or with two Faraday mirrors which selectively absorb one of the polarizations of two cavity modes ω_1 and ω_2. We parametrize the frequency difference in terms of $\omega_2 = \gamma\omega_1$ where $\gamma \in \mathbb{R}^+$ resulting in $\omega_{R(L)} = \sqrt{\omega_{1(2)}^2 + \omega_D^2}$. One of our central results is that the Berry phase at a light-matter hybridization can be predicted by

$$\frac{\phi_{\mathrm{p},l}}{2\pi} = \langle a_L^\dagger a_L\rangle_l^{k_f} - \langle a_L^\dagger a_L\rangle_l^{k_i} - \left(\langle a_R^\dagger a_R\rangle_l^{k_f} - \langle a_R^\dagger a_R\rangle_l^{k_i}\right). \quad (8)$$

This gives rise to four different cases in the prediction of the Berry phases at the avoided crossings, two of which are enlarged in Figs. 2(f) and 2(g). As depicted with a square in Figs. 2(b) and 2(c), at an avoided crossing between $l = 5$ and $l = 6$, two photons with opposite chiralities are exchanged with matter leading to a zero Berry phase $\phi_{\mathrm{p},5} = \phi_{\mathrm{p},6} = 0$, and hence a trivial gap. Depicted with a rhombus in Figs. 2(b) and 2(c), at an avoided crossing between $l = 4$ and $l = 5$ a photon changes chirality through the interactions with matter leading to $\phi_{\mathrm{p},4} = 2\pi[(1-0)-(0-1)] = 4\pi$ and $\phi_{\mathrm{p},5} = -4\pi$ Berry phase. In a simpler avoided crossing where a photon of fixed polarization is not exchanged at all, e.g., a left circularly polarized photon for band $l = 2$ in Figs. 2(b) and 2(c), The Berry phase is contributed only by an exchange between a right circularly polarized photon and matter, thus reproducing the single-polarization limit.

Therefore, Chern insulator phases with higher Chern numbers can be engineered by utilizing chiral photonic fields. This mechanism seems very general, and not restricted to graphene. For instance, high Chern numbers were reported in transition metal dichalcogenides coupled to a single-polarization cavity field [58]. Furthermore, the topological bands of the bulk suggest chiral edge modes with electron-photon localized states [56]. Our observation of high Chern numbers might also suggest larger photoelectron currents at the edges, or the domain walls, of the sample which could lend itself to device applications.

Discussion and outlook. Our analytical theory reveals cavity-mediated electronic interactions in graphene. This

analytical method is valid when $v_F g_\lambda/\omega_\lambda \ll 1$ and $k \ll \omega_\lambda/v_F$ hold [50], and the derived equations can only capture the physics at the Dirac gaps. The photon field fluctuations and light-matter entanglement cannot be neglected beyond these limits which include the topological light-matter hybridizations found away from the $\mathbf{K}$, $\mathbf{K}'$ points in high-energy bands. Hence in these cases, when the photonic Hilbert space is integrated out, one needs to resort to an open-system formalism for the electrons on which the numerical results can be found in the SM [50]. An analytical method to treat these hybridization points is an exciting future direction. Furthermore, understanding the competition of these cavity-mediated interactions with Coulomb interactions in strongly correlated electronic systems, e.g., moiré materials [59], is a promising path forward in the cavity-QED engineering of quantum materials.

Acknowledgments. We are grateful to Ashvin Vishwanath for many fruitful and guiding discussions on this work. The authors additionally thank Tilman Esslinger, Mohammad Hafezi, P. Myles Eugenio, Dan Parker, Pavel Volkov, and Jie Wang for stimulating discussions, and Oriana Diessel and Volker Karle for helpful comments on the paper. The authors acknowledge support from the NSF Award No. 2116679 through a grant for ITAMP at Harvard University.

[1] T. Oka and S. Kitamura, Annu. Rev. Condens. Matter Phys. **10**, 387 (2019).
[2] A. de la Torre, D. M. Kennes, M. Claassen, S. Gerber, J. W. McIver, and M. A. Sentef, Rev. Mod. Phys. **93**, 041002 (2021).
[3] T. Oka and H. Aoki, Phys. Rev. B **79**, 081406(R) (2009).
[4] N. H. Lindner, G. Refael, and V. Galitski, Nat. Phys. **7**, 490 (2011).
[5] T. Kitagawa, T. Oka, A. Brataas, L. Fu, and E. Demler, Phys. Rev. B **84**, 235108 (2011).
[6] D. Hsieh, F. Mahmood, J. W. McIver, D. R. Gardner, Y. S. Lee, and N. Gedik, Phys. Rev. Lett. **107**, 077401 (2011).
[7] J. McIver, D. Hsieh, H. Steinberg, P. Jarillo-Herrero, and N. Gedik, Nat. Nanotechnol. **7**, 96 (2012).
[8] Y. H. Wang, H. Steinberg, P. Jarillo-Herrero, and N. Gedik, Science **342**, 453 (2013).
[9] F. Mahmood, C.-K. Chan, Z. Alpichshev, D. Gardner, Y. Lee, P. A. Lee, and N. Gedik, Nat. Phys. **12**, 306 (2016).
[10] J. W. McIver, B. Schulte, F.-U. Stein, T. Matsuyama, G. Jotzu, G. Meier, and A. Cavalleri, Nat. Phys. **16**, 38 (2020).
[11] S. Zhou, C. Bao, B. Fan, H. Zhou, Q. Gao, H. Zhong, T. Lin, H. Liu, P. Yu, P. Tang *et al.*, Nature (London) **614**, 75 (2023).
[12] F. J. Garcia-Vidal, C. Ciuti, and T. W. Ebbesen, Science **373**, eabd0336 (2021).
[13] F. Schlawin, D. M. Kennes, and M. A. Sentef, Appl. Phys. Rev. **9**, 011312 (2022).
[14] P. Forn-Díaz, L. Lamata, E. Rico, J. Kono, and E. Solano, Rev. Mod. Phys. **91**, 025005 (2019).
[15] J. Flick, M. Ruggenthaler, H. Appel, and A. Rubio, Proc. Natl. Acad. Sci. USA **112**, 15285 (2015).
[16] H. Hübener, U. De Giovannini, C. Schäfer, J. Andberger, M. Ruggenthaler, J. Faist, and A. Rubio, Nat. Mater. **20**, 438 (2021).
[17] M. Ruggenthaler, D. Sidler, and A. Rubio, arXiv:2211.04241.
[18] D. Sidler, M. Ruggenthaler, C. Schäfer, E. Ronca, and A. Rubio, J. Chem. Phys. **156**, 230901 (2022).
[19] O. V. Kibis, O. Kyriienko, and I. A. Shelykh, Phys. Rev. B **84**, 195413 (2011).
[20] O. V. Kibis, Phys. Rev. B **81**, 165433 (2010).
[21] X. Wang, E. Ronca, and M. A. Sentef, Phys. Rev. B **99**, 235156 (2019).
[22] K. Masuki and Y. Ashida, Phys. Rev. B **107**, 195104 (2023).
[23] V. Rokaj, M. Ruggenthaler, F. G. Eich, and A. Rubio, Phys. Rev. Res. **4**, 013012 (2022).
[24] G. Scalari, C. Maissen, D. Turčinková, D. Hagenmüller, S. De Liberato, C. Ciuti, C. Reichl, D. Schuh, W. Wegscheider, M. Beck *et al.*, Science **335**, 1323 (2012).
[25] J. Keller, G. Scalari, F. Appugliese, S. Rajabali, M. Beck, J. Haase, C. A. Lehner, W. Wegscheider, M. Failla, M. Myronov *et al.*, Phys. Rev. B **101**, 075301 (2020).
[26] X. Li, M. Bamba, Q. Zhang, S. Fallahi, G. C. Gardner, W. Gao, M. Lou, K. Yoshioka, M. J. Manfra, and J. Kono, Nat. Photon. **12**, 324 (2018).
[27] D. Hagenmüller, S. De Liberato, and C. Ciuti, Phys. Rev. B **81**, 235303 (2010).
[28] N. Bartolo and C. Ciuti, Phys. Rev. B **98**, 205301 (2018).
[29] V. Rokaj, J. Wang, J. Sous, M. Penz, M. Ruggenthaler, and A. Rubio, Phys. Rev. Lett. **131**, 196602 (2023).
[30] Z. Bacciconi, G. M. Andolina, and C. Mora, Phys. Rev. B **109**, 165434 (2024).
[31] G. L. Paravicini-Bagliani, F. Appugliese, E. Richter, F. Valmorra, J. Keller, M. Beck, N. Bartolo, C. Rössler, T. Ihn, K. Ensslin *et al.*, Nat. Phys. **15**, 186 (2019).
[32] F. Appugliese, J. Enkner, G. L. Paravicini-Bagliani, M. Beck, C. Reichl, W. Wegscheider, G. Scalari, C. Ciuti, and J. Faist, Science **375**, 1030 (2022).
[33] G. Jarc, S. Y. Mathengattil, A. Montanaro, F. Giusti, E. M. Rigoni, R. Sergo, F. Fassioli, S. Winnerl, S. Dal Zilio, D. Mihailovic, P. Prelovšek, M. Eckstein, and D. Fausti, Nature (London) **622**, 487 (2023).
[34] M. P. Faraday, Philos. Trans. R. Soc. **136**, 1 (1846).
[35] J. Suits, IEEE Trans. Magn. **8**, 95 (1972).
[36] T. Arikawa, X. Wang, A. A. Belyanin, and J. Kono, Opt. Express **20**, 19484 (2012).
[37] J. Y. Chin, T. Steinle, T. Wehlus, D. Dregely, T. Weiss, V. I. Belotelov, B. Stritzker, and H. Giessen, Nat. Commun. **4**, 1599 (2013).
[38] K. J. Carothers, R. A. Norwood, and J. Pyun, Chem. Mater. **34**, 2531 (2022).
[39] E. Plum and N. I. Zheludev, Appl. Phys. Lett. **106**, 221901 (2015).
[40] M. S. Rudner and J. C. W. Song, Nat. Phys. **15**, 1017 (2019).
[41] K. P. Nuckolls, M. Oh, D. Wong, B. Lian, K. Watanabe, T. Taniguchi, B. A. Bernevig, and A. Yazdani, Nature (London) **588**, 610 (2020).
[42] J. M. Luttinger and W. Kohn, Phys. Rev. **97**, 869 (1955).
[43] J. R. Schrieffer and P. A. Wolff, Phys. Rev. **149**, 491 (1966).

[44] N. Rivera, J. Sloan, Y. Salamin, J. D. Joannopoulos, and M. Soljačić, Proc. Natl. Acad. Sci. USA **120**, e2219208120 (2023).
[45] A. Kundu, H. A. Fertig, and B. Seradjeh, Phys. Rev. Lett. **113**, 236803 (2014).
[46] P. M. Perez-Piskunow, L. E. F. Foa Torres, and G. Usaj, Phys. Rev. A **91**, 043625 (2015).
[47] G. Usaj, P. M. Perez-Piskunow, L. E. F. Foa Torres, and C. A. Balseiro, Phys. Rev. B **90**, 115423 (2014).
[48] M. A. Sentef, J. Li, F. Künzel, and M. Eckstein, Phys. Rev. Res. **2**, 033033 (2020).
[49] B. A. Bernevig, *Topological Insulators and Topological Superconductors* (Princeton University Press, Princeton, NJ, 2013).
[50] See Supplemental Material at http://link.aps.org/supplemental/10.1103/PhysRevB.110.L121101 for the derivation of a tight-binding model for graphene coupled to a chiral cavity, Berry curvature and Chern number results, arguments on the time-reversal symmetry breaking, derivation of the Schrieffer-Wolff effective Hamiltonians with a convergence analysis, Hartree-Fock mean-field theory calculations, and density-matrix Chern value formalism for mixed electronic states, which includes Refs. [60–70].
[51] Y. Zhang, Y.-W. Tan, H. L. Stormer, and P. Kim, Nature (London) **438**, 201 (2005).
[52] C. Maissen, G. Scalari, F. Valmorra, M. Beck, J. Faist, S. Cibella, R. Leoni, C. Reichl, C. Charpentier, and W. Wegscheider, Phys. Rev. B **90**, 205309 (2014).
[53] Y. Cao, V. Fatemi, A. Demir, S. Fang, S. L. Tomarken, J. Y. Luo, J. D. Sanchez-Yamagishi, K. Watanabe, T. Taniguchi, E. Kaxiras, R. C. Ashoori, and P. Jarillo-Herrero, Nature (London) **556**, 80 (2018).
[54] J. A. Sobota, Y. He, and Z.-X. Shen, Rev. Mod. Phys. **93**, 025006 (2021).
[55] T. Fukui, Y. Hatsugai, and H. Suzuki, J. Phys. Soc. Jpn. **74**, 1674 (2005).
[56] T. Karzig, C.-E. Bardyn, N. H. Lindner, and G. Refael, Phys. Rev. X **5**, 031001 (2015).
[57] D. G. Suárez-Forero, R. Ni, S. Sarkar, M. J. Mehrabad, E. Mechtel, V. Simonyan, A. Grankin, K. Watanabe, T. Taniguchi, S. Park, H. Jang, M. Hafezi, and Y. Zhou, arXiv:2308.04574.
[58] D.-P. Nguyen, G. Arwas, Z. Lin, W. Yao, and C. Ciuti, Phys. Rev. Lett. **131**, 176602 (2023).
[59] E. Y. Andrei, D. K. Efetov, P. Jarillo-Herrero, A. H. MacDonald, K. F. Mak, T. Senthil, E. Tutuc, A. Yazdani, and A. F. Young, Nat. Rev. Mater. **6**, 201 (2021).
[60] F. D. M. Haldane, Phys. Rev. Lett. **61**, 2015 (1988).
[61] H. Spohn, *Dynamics of Charged Particles and their Radiation Field* (Cambridge University Press, Cambridge, UK, 2004).
[62] C. Cohen-Tannoudji, J. Dupont-Roc, and G. Grynberg, *Photons and Atoms—Introduction to Quantum Electrodynamics* (Wiley-VCH, Weinheim, Germany, 1997).
[63] K. F. Mak and J. Shan, Nat. Nanotechnol. **17**, 686 (2022).
[64] V. Rokaj, D. M. Welakuh, M. Ruggenthaler, and A. Rubio, J. Phys. B: At. Mol. Opt. Phys. **51**, 034005 (2018).
[65] R. Luo, G. Benenti, G. Casati, and J. Wang, Phys. Rev. Res. **2**, 022009(R) (2020).
[66] G. Baym, *Lectures on Quantum Mechanics* (W. A. Benjamin Inc., New York, 1969).
[67] N. W. Aschroft and N. Mermin, *Solid State Physics* (Saunders College Publishing, Philadelphia, 1976).
[68] C. Bena and G. Montambaux, New J. Phys. **11**, 095003 (2009).
[69] S. Hu and S. M. Weiss, ACS Photon. **3**, 1647 (2016).
[70] A. Rivas, O. Viyuela, and M. A. Martin-Delgado, Phys. Rev. B **88**, 155141 (2013).